ISSN 0915-633X

INTERNATIONAL ATOMIC ENERGY AGENCY

SIXTEENTH IAEA FUSION ENERGY CONFERENCE

Montréal, Canada, 7-11 October 1996

IAEA-CN-64/CP-5

NATIONAL INSTITUTE FOR FUSION SCIENCE

Dynamics of Ion Temperature in Heliotron-E

K. Ida, K. Kondo, K. Nagasaki T. Hamada, H. Zushi,
S. Hidekuma, F. Sano, T. Mizuuchi, H. Okada,
S. Besshou, H. Funaba, Y. Kurimoto,
K. Watanabe and T. Obiki

(Received - Aug. 26, 1996)

NIFS-439 Sep. 1996

RESEARCH REPORT
NIFS Series

NAGOYA, JAPAN

DYNAMICS OF ION TEMPERATURE IN HELIOTRON-E

K.IDA[1], K.KONDO[2], K.NAGASAKI[3], T.HAMADA[4], H.ZUSHI[2],
S.HIDEKUMA[1], F.SANO[3], T.MIZUUCHI[3], H.OKADA[3],
S.BESSHOU[2], H.FUNABA[4], Y.KURIMOTO[4], K.WATANABE[1],
T.OBIKI[3]

[1]National Institute for Fusion Science,
Nagoya, 464-01, Japan

[2]Graduate School of Energy Science,
Kyoto University,
Uji, 611, Japan

[3]Institute of Advanced Energy,
Kyoto University,
Uji, 611, Japan

[4]Faculty of Engineering,
Kyoto University,
Kyoto, 606-01, Japan.

Keywords: Radial Electric Field, Heliotron-E, Charge Exchange Spectroscopy,
Pellet Injection

Abstract

Ion temperature dynamics related with the density profile are studied in Heliotron-E plasma. The density profiles can be peaked by the H_2/D_2 pellet injection or flattened by second harmonic electron cyclotron heating (2nd-ECH). Higher ion temperature and better ion transport are observed associated with the density peaking, and a large density gradient results in the radial electric field shear. The improvement of ion transport is more related to the radial electric field shear, rather than to the bulk velocity shear.

1. INTRODUCTION

Ion temperature dynamics are studied for neutral beam heated plasmas with H2/D2 pellet injection and/or second harmonic electron cyclotron heating (2nd-ECH) in Heliotron E. Heliotron-E is an axially asymmetric heliotron/torsatron with l=2 , m=19, major radius R=2.2m, minor radius a = 0.2m, magnetic field B=1.9T, NBI power < 3MW [1]. The time evolution of ion temperature profiles are measured with multi-chord charge exchange spectroscopy (TVCXS) with 40 spatial channels and with a 16.7ms time resolution using a charge exchange recombination line of fully stripped carbon [2]. Fast changes in the central ion temperature are measured with a center chord neutral particle analyzer (NPA) with the time resolution of 2 ms. The density peakedness is estimated with 7-chord FIR interferometer [3].

2. PELLET INJECTION

As shown in Fig.1(a), the central ion temperature keeps increasing after recovering from the H2/D2 pellet injection and the central ion temperature doubles well after the pellet injection (> 50 ms). The electron density profile becomes hollow with pellet injection (t=332ms), because the pellet penetrates only to half of the plasma minor radius. The density profile is peaked in a few tens of ms after the pellet injection and becomes even more peaked afterwards (t=408ms). Figure 1(b) shows the peaking factor of ion temperature profiles as a function of the peaking factor of electron density profiles plotted every

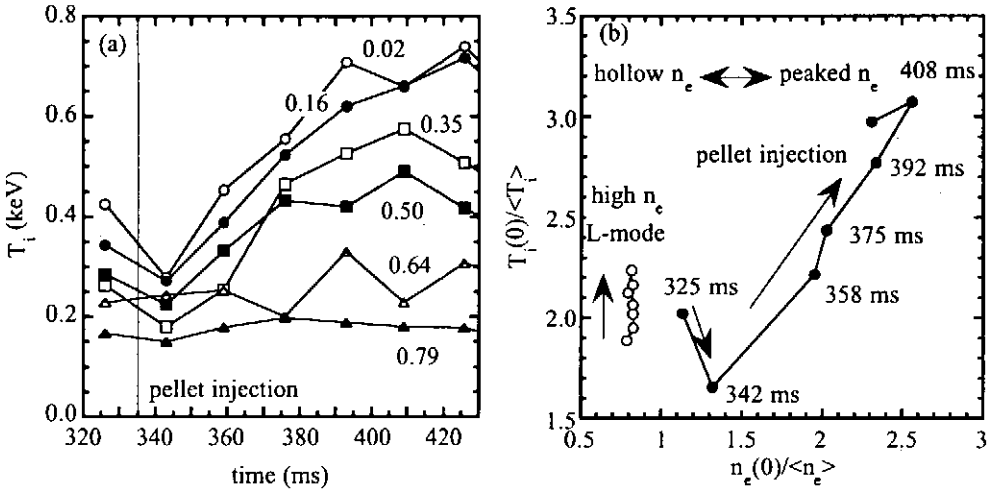

FIG.1 (a)Time evolution of the ion temperature at r = 0.02, 0.16, 0.35, 0.50, 0.64 and 0.79 measured with TVCXS and (b) peaking factor of ion temperature profiles as function of peaking factor of electron density profiles for the L-mode discharges and discharges with pellet injection in the Heliotron-E.

16.7ms for the pellet injection discharges and also, for reference, the L-mode discharges with similar central electron density. It clearly shows the strong coupling of ion temperature peaking and electron density peaking. The strong coupling of ion temperature peaking and electron density peaking ($T_i(0)/<T_i>$ = 3.1 and $n_e(0)/<n_e>$ = 2.6, where <> stands for volume average) and improvement of ion transport due to density gradient are also observed in high T_i mode discharges [4], where the spontaneous density and temperature peaking occurs after the NBI with no gas puff and with low wall recycling due to boron coating.

One of the effects of density peaking is to enhance the radial electric field, if the bulk rotation is kept constant. To check that, the radial electric field profiles are derived from the impurity poloidal rotation profiles with a radial force balance equation of impurities. From the radial force balance, the force due to the radial electric field, E_r, should be balanced by the forces due to the pressure gradient and the Lorentz force due to plasma rotation as $E_r = (1/eZ_in_i)\partial p_i/\partial r + (B_\theta v_\phi - B_\phi v_\theta)$, where p is pressure, B_θ and B_ϕ are the poloidal and toroidal magnetic field, and v_θ and v_ϕ are the poloidal and toroidal rotation velocity. The suffix i stands for species and i=H for bulk hydrogen and

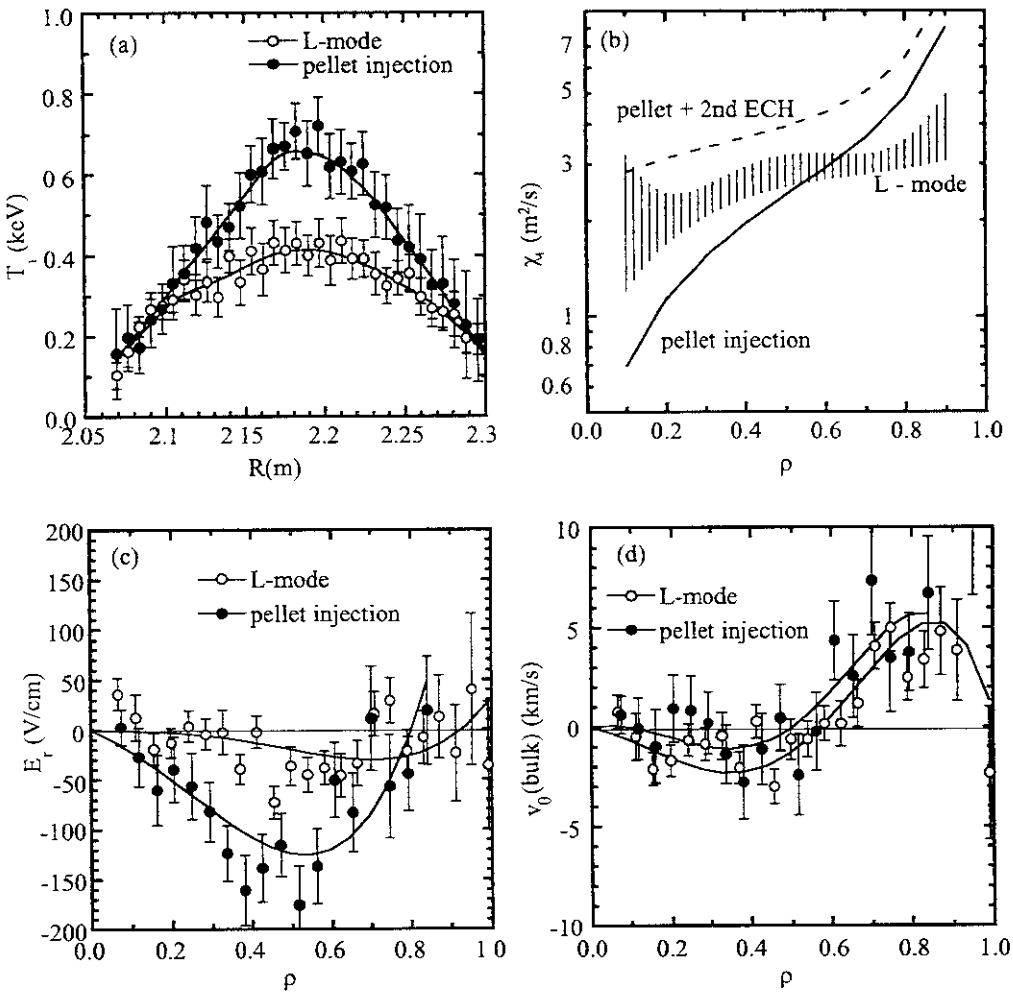

FIG.2. Radial profiles of (a) ion temperature, (b) ion thermal diffusivity, (c) radial electric field, and (d) bulk poloidal rotation velocity for the L-mode discharges and the discharges with pellet injection ($n_e(0) = 7.3 \times 10^{19}/m^3$) in the Heliotron-E.

i=C for carbon impurity. Z_i is atomic charge of bulk (Z_H =1) or carbon impurities (Z_C =6). In the heliotron/torsatron devices, toroidal rotation is damped by parallel viscosity, $v_\phi \sim 0$, then $E_r \sim (1/eZ_in_i)\partial p_i/\partial r - B_\phi v_{\theta i}$. Poloidal rotation profiles of impurity ions, $v_{\theta C}(R)$, are measured and the radial electric field, E_r, is calculated with $E_r = (1/eZ_Cn_C)\partial p_C/\partial r - B_\phi v_{\theta C}$. The bulk poloidal rotation velocity is estimated from the radial electric field and bulk pressure gradient measured as $v_{\theta H} = (1/eB_\phi Z_H n_H)\partial p_H/\partial r - E_r/B_\phi$. Here it should be noted that the diamagnetic drift velocity of the bulk ions $(1/eB_\phi Z_H n_H)\partial p_H/\partial r$ is

comparable to the E_r/B_ϕ drift velocity. On the other hand, the diamagnetic drift velocity of the carbon impurity $(1/eB_\phi Z_C n_C)\partial p_C/\partial r$ is much smaller than the E_r/B_ϕ drift velocity.

As shown in Figs. 2, a more negative radial electric field and greater E_r shear are observed in the pellet injection mode than in the L-mode discharges, although the bulk poloidal rotation velocity profile in the pellet injection mode is similar to that in the L-mode discharge. The peaked ion temperature profiles with the pellet injection is due to the improved ion transport (as seen in the ion thermal diffusivity profiles) The improvement of ion transport can be explained by the radial electric field shear due to the large density gradient (density peaking) triggered by pellet injection. The largest improvement of ion transport is observed near the plasma center, not outside the half plasma minor radius, where the radial electric field has its maximum magnitude. Therefore these results suggest that E_r shear is more important than the bulk plasma velocity shear in reducing the turbulence and improving ion transport.

3. SECOND HARMONIC ECH

Second harmonic ECH has particle "pump-out" in the core region and makes the density profiles flat [5]. When the 2nd-ECH is applied to the plasma with peaked density profile, both the density peakedness and central ion temperature decrease, although the total heating power by NBI plus ECH is increased [6]. To study a causal link between the radial electric field shear due to density gradient and improvement of ion transport, time evolution of the density peakedness and the central ion temperature are measured at the onset of the 2nd-ECH pulse for the high T_i mode discharges, where both the electron density and ion temperature are peaked. As seen in Fig. 3(a), the central ion temperature starts to decrease after the 2nd-ECH pulse is turned on and recovers after the ECH pulse is turned off. These changes in the central ion temperature are associated with the flattening of the density profile.

Figure 3(b) shows the central ion temperature as a function of the density peaking factor. If the density flattening (decrease of radial electric field shear) and drop of central ion temperature take place simultaneously, this is the case that 2nd harmonic ECH directly deteriorate both particle and heat transport, the time trace should be on one line. When there is causality between these two

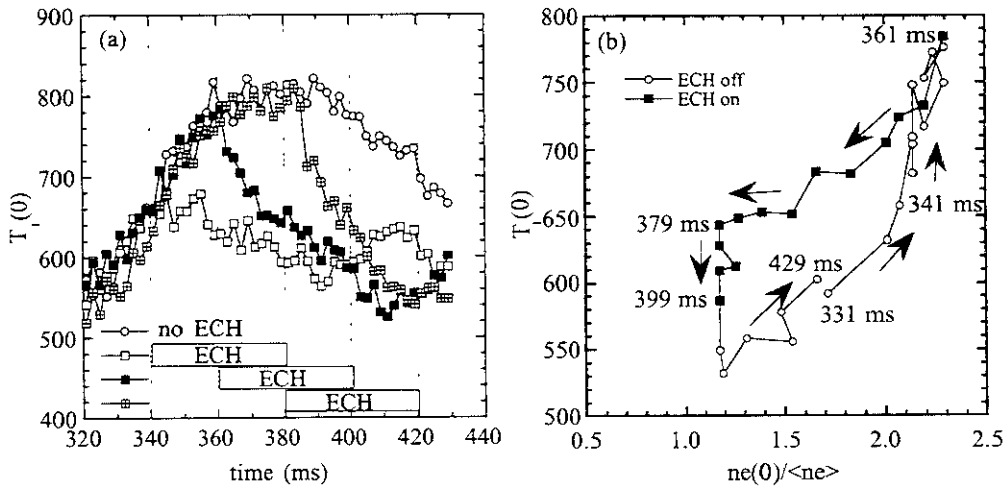

FIG.3. (a)Time evolution of the ion temperature measured with neutral particle analyzer (NPA) for the high T_i mode discharge (no ECH pulse) and the discharges with 2nd harmonic ECH pulse for t = 340-360ms, 360-400ms, and 380-420ms and (b) central ion temperature profiles as a function of peaking factor of electron density profiles for the discharge with 2nd harmonic ECH pulse for t = 360-400ms in the Heliotron-E.

parameters, the time trace deforms to be elongated circularly and the direction of rotation (clockwise or counter clockwise) shows which is first. The measured data clearly shows that the change of density peaking factor is first. These observations support the hypothesis that the density gradient and radial electric field shear contribute to the improvement of ion transport. The flattening of density profiles causes the drop in ion temperature and the enhancement of the ion thermal diffusivity. The large ion thermal diffusivity for the discharges with a 2nd ECH pulse [see Fig.2(b)] is also explained by this mechanism.

4. CONCLUSION

Dynamics of ion temperaure for the density peaking phase shows that the increase in density gradient, which produces larger radial electric field shear, causes the increase of ion temperature due to the reduction of ion thermal diffusivity. Most L-mode discharges in Heliotron-E have flat electron density and small E_r shear and that result in a flat ion temperature profile (typically less peaked than that in tokamak). However, by controlling E_r shear (not bulk

poloidal rotation shear) with pellet injection through density peaking, the ion thermal diffusivity, χ_i, can be reduced to 0.7 m^2/s at $\rho = 0.1$, which value is in between the χ_i values for L-mode and those for the improved modes ($\chi_i(0.1)$ = $0.5m^2/s$ in supershot , $\chi_{eff}(0.2) = 0.6m^2/s$ in PEP-mode, $\chi_{eff}(0.2) = 0.4m^2/s$ in VH-mode, $\chi_i(0.1) = 0.1m^2/s$ in high-β_p mode) in tokamaks [7-10]. On the other hand, the 2nd harmonic ECH deteriorates the density peaking and enhances the ion thermal diffusivity (≈ 3 m^2/s) as high as or even higher than that in L- mode discharges.

REFERENCES

[1] SANO, F., et. al., Nucl. Fusion **30** (1990) 81.

[2] IDA, K., HIDEKUMA, S., Rev. Sci. Instrum. **60**, (1989) 867.

[3] ZUSHI, H., et al., Nucl. Fusion **27** (1987) 286.

[4] IDA, K., et al., Phys. Rev. Lett. **76** (1996) 1268.

[5] MIZUUCHI, T., et al., to be published in Controlled Fusion and Plasma Physics (Proc. 23rd Eur. Conf. Kiev, 1996) European Physical Society.

[6] OBIKI, T.,this conference.

[7] HAWRYLUK, R.J., et al., Plasma Phys. Control. Fusion **33** (1991) 1509.

[8] KEILHACKER, M., et al., Plasma Phys. Control. Fusion **33** (1991) 1453.

[9] OSBONE, T.H., et al., Plasma Phys. Control. Fusion **36** (1994) A237.

[10] SHIRAI, H., et al., in Plasma Physics and Controlled Nuclear Fusion Research (Proc. 15th Int. Conf., Seville, 1994), Vol.1, IAEA, Vienna (1995) 355.

Recent Issues of NIFS Series

NIFS-397 H. Kuramoto, N. Hiraki, S. Moriyama, K. Toi, K. Sato, K. Narihara, A. Ejiri, T. Seki and JIPP T-IIU Group,
Measurement of the Poloidal Magnetic Field Profile with High Time Resolution Zeeman Polarimeter in the JIPP T-IIU Tokamak; Feb. 1996

NIFS-398 J.F. Wang, T. Amano, Y. Ogawa, N. Inoue,
Simulation of Burning Plasma Dynamics in ITER; Feb. 1996

NIFS-399 K. Itoh, S-I. Itoh, A. Fukuyama and M. Yagi,
Theory of Self-Sustained Turbulence in Confined Plasmas; Feb. 1996

NIFS-400 J. Uramoto,
A Detection Method of Negative Pionlike Particles from a H2 Gas Descharge Plasma; Feb. 1996

NIFS-401 K.Ida, J.Xu, K.N.Sato, H.Sakakita and JIPP TII-U group,
Fast Charge Exchange Spectroscopy Using a Fabry-Perot Spectrometer in the JIPP TII-U Tokamak; Feb. 1996

NIFS-402 T. Amano,
Passive Shut-Down of ITER Plasma by Be Evaporation; Feb. 1996

NIFS-403 K. Orito,
A New Variable Transformation Technique for the Nonlinear Drift Vortex; Feb. 1996

NIFS-404 T. Oike, K. Kitachi, S. Ohdachi, K. Toi, S. Sakakibara, S. Morita, T. Morisaki, H. Suzuki, S. Okamura, K. Matsuoka and CHS group; *Measurement of Magnetic Field Fluctuations near Plasma Edge with Movable Magnetic Probe Array in the CHS Heliotron/Torsatron*; Mar. 1996

NIFS-405 S.K. Guharay, K. Tsumori, M. Hamabe, Y. Takeiri, O. Kaneko, T. Kuroda,
Simple Emittance Measurement of H- Beams from a Large Plasma Source; Mar. 1996

NIFS-406 M. Tanaka and D. Biskamp,
Symmetry-Breaking due to Parallel Electron Motion and Resultant Scaling in Collisionless Magnetic Reconnection; Mar. 1996

NIFS-407 K. Kitachi, T. Oike, S. Ohdachi, K. Toi, R. Akiyama, A. Ejiri, Y. Hamada, H.Kuramoto, K. Narihara, T. Seki and JIPP T-IIU Group,
Measurement of Magnetic Field Fluctuations within Last Closed Flux Surface with Movable Magnetic Probe Array in the JIPP T-IIU Tokamak; Mar. 1996

NIFS-408 K. Hirose, S. Saito and Yoshi.H. Ichikawa

Structure of Period-2 Step-1 Accelerator Island in Area Preserving Maps; Mar. 1996

NIFS-409 G.Y.Yu, M. Okamoto, H. Sanuki, T. Amano,
Effect of Plasma Inertia on Vertical Displacement Instability in Tokamaks; Mar. 1996

NIFS-410 T. Yamagishi,
Solution of Initial Value Problem of Gyro-Kinetic Equation; Mar. 1996

NIFS-411 K. Ida and N. Nakajima,
Comparison of Parallel Viscosity with Neoclassical Theory; Apr. 1996

NIFS-412 T. Ohkawa and H. Ohkawa,
Cuspher, A Combined Confinement System; Apr. 1996

NIFS-413 Y. Nomura, Y.H. Ichikawa and A.T. Filippov,
Stochasticity in the Josephson Map; Apr. 1996

NIFS-414 J. Uramoto,
Production Mechanism of Negative Pionlike Particles in H_2 Gas Discharge Plasma; Apr. 1996

NIFS-415 A. Fujisawa, H. Iguchi, S. Lee, T.P. Crowley, Y. Hamada, S. Hidekuma, M. Kojima,
Active Trajectory Control for a Heavy Ion Beam Probe on the Compact Helical System; May 1996

NIFS-416 M. Iwase, K. Ohkubo, S. Kubo and H. Idei
Band Rejection Filter for Measurement of Electron Cyclotron Emission during Electron Cyclotron Heating; May 1996

NIFS-417 T. Yabe, H. Daido,T. Aoki, E. Matsunaga and K. Arisawa,
Anomalous Crater Formation in Pulsed-Laser-Illuminated Aluminum Slab and Debris Distribution; May 1996

NIFS-418 J. Uramoto,
Extraction of K^- Mesonlike Particles from a D_2 Gas Discharge Plasma in Magnetic Field; May 1996

NIFS-419 J. Xu, K. Toi, H. Kuramoto, A. Nishizawa, J. Fujita, A. Ejiri, K. Narihara, T. Seki, H. Sakakita, K. Kawahata, K. Ida, K. Adachi, R. Akiyama, Y. Hamada, S. Hirokura, Y. Kawasumi, M. Kojima, I. Nomura, S. Ohdachi, K.N. Sato
Measurement of Internal Magnetic Field with Motional Stark Polarimetry in Current Ramp-Up Experiments of JIPP T-IIU; June 1996

NIFS-420 Y.N. Nejoh,
Arbitrary Amplitude Ion-acoustic Waves in a Relativistic Electron-beam

Plasma System; July 1996

NIFS-421 K. Kondo, K. Ida, C. Christou, V.Yu.Sergeev, K.V.Khlopenkov, S.Sudo, F. Sano, H. Zushi, T. Mizuuchi, S. Besshou, H. Okada, K. Nagasaki, K. Sakamoto, Y. Kurimoto, H. Funaba, T. Hamada, T. Kinoshita, S. Kado, Y. Kanda, T. Okamoto, M. Wakatani and T. Obiki,
Behavior of Pellet Injected Li Ions into Heliotron E Plasmas; July 1996

NIFS-422 Y. Kondoh, M. Yamaguchi and K. Yokozuka,
Simulations of Toroidal Current Drive without External Magnetic Helicity Injection; July 1996

NIFS-423 Joong-San Koog,
Development of an Imaging VUV Monochromator in Normal Incidence Region. July 1996

NIFS-424 K. Orito,
A New Technique Based on the Transformation of Variables for Nonlinear Drift and Rossby Vortices; July 1996

NIFS-425 A. Fujisawa, H. Iguchi, S. Lee, T.P. Crowley, Y. Hamada, H. Sanuki, K. Itoh, S. Kubo, H. Idei, T. Minami, K. Tanaka, K. Ida, S. Nishimura, S. Hidekuma, M. Kojima, C. Takahashi, S. Okamura and K. Matsuoka,
Direct Observation of Potential Profiles with a 200keV Heavy Ion Beam Probe and Evaluation of Loss Cone Structure in Toroidal Helical Plasmas on the Compact Helical System; July 1996

NIFS-426 H. Kitauchi, K. Araki and S. Kida,
Flow Structure of Thermal Convection in a Rotating Spherical Shell; July 1996

NIFS-427 S. Kida and S. Goto,
Lagrangian Direct-interaction Approximation for Homogeneous Isotropic Turbulence; July 1996

NIFS-428 V.Yu. Sergeev, K.V. Khlopenkov, B.V. Kuteev, S. Sudo, K. Kondo, F. Sano, H. Zushi, H. Okada, S. Besshou, T. Mizuuchi, K. Nagasaki, Y. Kurimoto and T. Obiki,
Recent Experiments on Li Pellet Injection into Heliotron E; Aug. 1996

NIFS-429 N. Noda, V. Philipps and R. Neu,
A Review of Recent Experiments on W and High Z Materials as Plasma-Facing Components in Magnetic Fusion Devices; Aug. 1996

NIFS-430 R.L. Tobler, A. Nishimura and J. Yamamoto,
Design-Relevant Mechanical Properties of 316-Type Stainless Steels for Superconducting Magnets; Aug. 1996

NIFS-431 K. Tsuzuki, M. Natsir, N. Inoue, A. Sagara, N. Noda, O. Motojima, T. Mochizuki, T. Hino and T. Yamashina,
Hydrogen Absorption Behavior into Boron Films by Glow Discharges in Hydrogen and Helium; Aug. 1996

NIFS-432 T.-H. Watanabe, T. Sato and T. Hayashi,
Magnetohydrodynamic Simulation on Co- and Counter-helicity Merging of Spheromaks and Driven Magnetic Reconnection; Aug. 1996

NIFS-433 R. Horiuchi and T. Sato,
Particle Simulation Study of Collisionless Driven Reconnection in a Sheared Magnetic Field; Aug. 1996

NIFS-434 Y. Suzuki, K. Kusano and K. Nishikawa,
Three-Dimensional Simulation Study of the Magnetohydrodynamic Relaxation Process in the Solar Corona. II.; Aug. 1996

NIFS-435 H. Sugama and W. Horton,
Transport Processes and Entropy Production in Toroidally Rotating Plasmas with Electrostatic Turbulence; Aug. 1996

NIFS-436 T. Kato, E. Rachlew-Källne, P. Hörling and K.-D Zastrow,
Observations and Modelling of Line Intensity Ratios of OV Multiplet Lines for 2s3s 3S1 - 2s3p 3Pj; Aug. 1996

NIFS-437 T. Morisaki, A. Komori, R. Akiyama, H. Idei, H. Iguchi, N. Inoue, Y. Kawai, S. Kubo, S. Masuzaki, K. Matsuoka, T. Minami, S. Morita, N. Noda, N. Ohyabu, S. Okamura, M. Osakabe, H. Suzuki, K. Tanaka, C. Takahashi, H. Yamada, I. Yamada and O. Motojima,
Experimental Study of Edge Plasma Structure in Various Discharges on Compact Helical System; Aug. 1996

NIFS-438 A. Komori, N. Ohyabu, S. Masuzaki, T. Morisaki, H. Suzuki, C. Takahashi, S. Sakakibara, K. Watanabe, T. Watanabe, T. Minami, S. Morita, K. Tanaka, S. Ohdachi, S. Kubo, N. Inoue, H. Yamada, K. Nishimura, S. Okamura, K. Matsuoka, O. Motojima, M. Fujiwara, A. Iiyoshi, C. C. Klepper, J.F. Lyon, A.C. England, D.E. Greenwood, D.K. Lee, D.R. Overbey, J.A. Rome, D.E. Schechter and C.T. Wilson,
Edge Plasma Control by a Local Island Divertor in the Compact Helical System; Sep. 1996 (IAEA-CN-64/C1-2)

NIFS-439 K. Ida, K. Kondo, K. Nagasaki T. Hamada, H. Zushi, S. Hidekuma, F. Sano, T. Mizuuchi, H. Okada, S. Besshou, H. Funaba, Y. Kurimoto, K. Watanabe and T. Obiki,
Dynamics of Ion Temperature in Heliotron-E; Sep. 1996 (IAEA-CN-64/CP-5)